Thin Solid Films 517 (2009) 2920–2923

Contents lists available at ScienceDirect

Thin Solid Films

journal homepage: www.elsevier.com/locate/tsf

Synthesis and characterization of Nb_2AlC thin films

T.H. Scabarozi [a,b], J. Roche [a], A. Rosenfeld [a], S.H. Lim [c], L. Salamanca-Riba [c], G. Yong [d], I. Takeuchi [c], M.W. Barsoum [b], J.D. Hettinger [a], S.E. Lofland [a,*]

[a] Department of Physics and Astronomy, Rowan University, Glassboro, NJ 08028, USA
[b] Department of Materials Science and Engineering, Drexel University, Philadelphia, PA 19104, USA
[c] Department of Materials Science and Engineering, University of Maryland, College Park, MD 20742, USA
[d] Department of Physics and Astronomy, Towson University,Towson, MD 21252, USA

ARTICLE INFO

Article history:
Received 6 June 2008
Received in revised form 6 December 2008
Accepted 17 December 2008
Available online 31 December 2008

Keywords:
Carbides
Sputtering
Superconductivity

ABSTRACT

We report on the synthesis and characterization of epitaxial *c*-axis oriented Nb_2AlC thin films deposited on *c*-axis sapphire (Al_2O_3) substrates by magnetron sputtering. Selected area electron diffraction reveal that independent of substrate temperature or film stoichiometry, there is the growth of a secondary phase not found in bulk, $Nb_5Al_3C_x$ with *a*- and *c*-axis lattice constants of 7.746 Å and 5.246 Å, respectively. Scanning electron micrographs reveal large surface features, many with hexagonal shape and faceted texture. Atomic force microscopy topographical measurements indicate a surface roughness of approximately 15% of the total film thickness. Electrical transport measurements show typical metal-like conduction with a room temperature resistivity of ≈0.9 μΩ-m and a residual resistivity ratio of 2.5. A superconducting transition was found at ≈440 mK.

1. Introduction

Ternary carbides and nitrides that follow the $M_{n+1}AX_n$ chemistry ($n=1, 2$ or 3), where M is a transition metal, A is an A-group element, and X is carbon and/or nitrogen, have drawn recent interest because of their unusual and sometimes unique properties [1–3]. These include high electrical and thermal conductivities and low coefficients of friction. The hexagonal structure consists of $M_{n+1}X_n$ layers interleaved by layers of the A-group element. The unusual combination of properties of these materials makes them candidates for applications, such as electronic contacts and protective coatings that require synthesis in thin-film form.

Growth of epitaxial MAX-phase films is becoming a mature area of research as demonstrated by the numerous publications on the synthesis and characterization of these films [4–9]. Oriented thin films should also provide insight to anisotropic properties of the material when compared directly to their bulk polycrystalline counterparts. Recent results have demonstrated that the anisotropy in the physical properties is not as large as expected and that low defect-concentration films have high charge mobilities that sometimes reveal new physics [10].

2. Experimental

Thin films were deposited in a custom built ultra-high vacuum magnetron sputtering chamber. Three magnetron cathodes housed individual two-inch elemental targets, which were about ~7 cm above the substrate. At deposition temperature, a base pressure of 5×10^{-8} Torr was achieved prior to each deposition. Films were deposited by radio-frequency sputtering in a sputtering grade Ar (99.9995%) atmosphere (50 sccm) at pressures ranging from 4–18 mTorr.

Substrates of MgO (111), Si (100), *c*- (00 l) and *r*-plane (012) sapphire (Al_2O_3), and polycrystalline Al_2O_3, were cleaned in acetone and methanol in an ultrasonic cleaner for 5 min prior to their placement in the chamber. Films were deposited in the temperature range of 700–1000 °C as determined by optical pyrometry. The substrate temperature was ramped at a rate of 35 °C/min to the desired temperature, where it was held for a minimum of 0.5 h prior to deposition. Films were deposited for 10–80 min at a deposition rate of ~7 nm/min.

Two-theta X-ray diffraction (XRD) was carried out with a Scintag X_2 diffractometer utilizing Cu-Kα radiation. 4-circle XRD was performed on a Bruker D8 Discover diffractometer utilizing Cu-Kα radiation. A JEOL JEM-2100F high-resolution field-emission transmission electron microscope (HRTEM) operating at 200 kV was used to investigate the interfaces and microstructure. Surface morphology and topography was investigated by scanning electron microscopy (SEM) with a LEO 1530VP field-emission microscope operating at 11 kV and by atomic force microscopy (AFM) with a JEOL SPM-5200 using a 10 nm diameter tip in both contact and non-contact modes with resonant frequencies of 25 and 300 kHz, respectively. Chemical analysis was performed by energy dispersive X-ray spectroscopy (EDS) with an EDAX Genesis detector on the SEM. Due to limitations of EDS only the Nb and Al elements were quantifiable.

Raman spectra were taken at room temperature with a Renishaw 2000 spectrometer with either an Ar-ion laser (514.5 nm) or HeNe laser

* Corresponding author.
E-mail address: lofland@rowan.edu (S.E. Lofland).

0040-6090/$ – see front matter © 2009 Elsevier B.V. All rights reserved.
doi:10.1016/j.tsf.2008.12.047

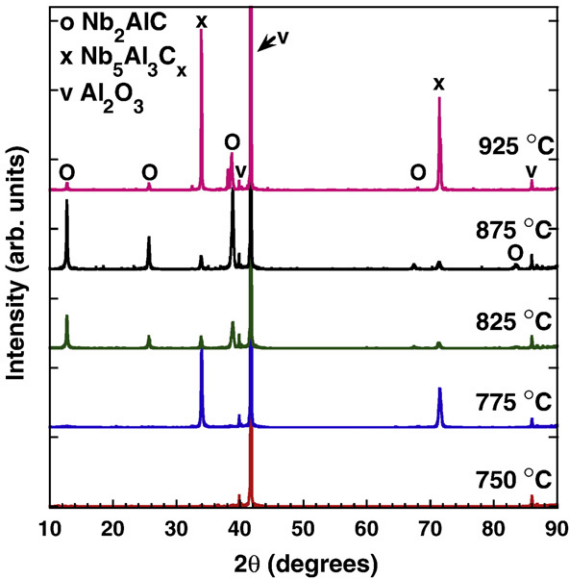

Fig. 1. X-ray diffraction pattern of Nb–Al–C films grown at various temperatures on *c*-axis sapphire. Curves are offset for clarity.

(633 nm). Spectra were collected in static mode over five accumulations with a 60-s exposure time for each accumulation. Experimental peak positions were calculated through Lorentzian fitting with a system resolution of 2 cm^{-1}.

Electrical transport measurements were carried out on 400-μm wide by 1.6-mm long microbridges that were defined by standard photolithographic techniques, followed by acid wet etch in $1HF+1HNO_3+1H_2O$. The resistivity was measured as a function of temperature T for $0.4\ K \le T \le 300\ K$ range with a Quantum Design Physical Properties Measurement System by a four-probe technique. The details of this experimental procedure can be found elsewhere [10–14].

3. Results and discussion

Since carbon content can only be qualitatively determined by EDS, carbon content was initially estimated by optimizing films of (111) NbC and (001) Nb_2C grown on *c*-plane sapphire at 850 °C. The power

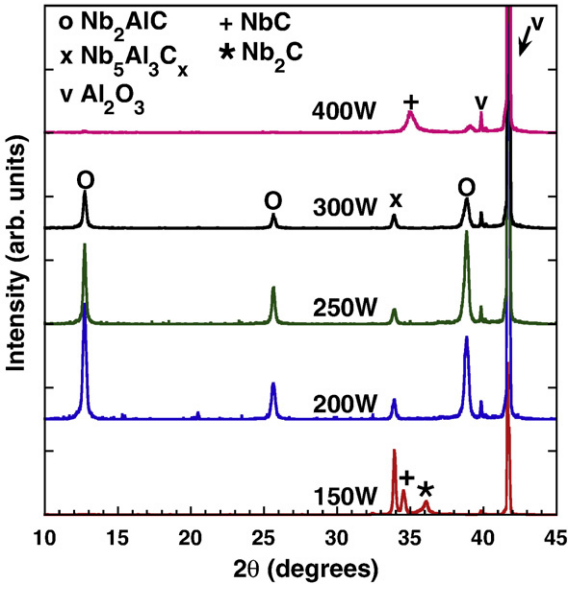

Fig. 2. X-ray diffraction patterns of films deposited at various carbon powers. Curves are offset for clarity.

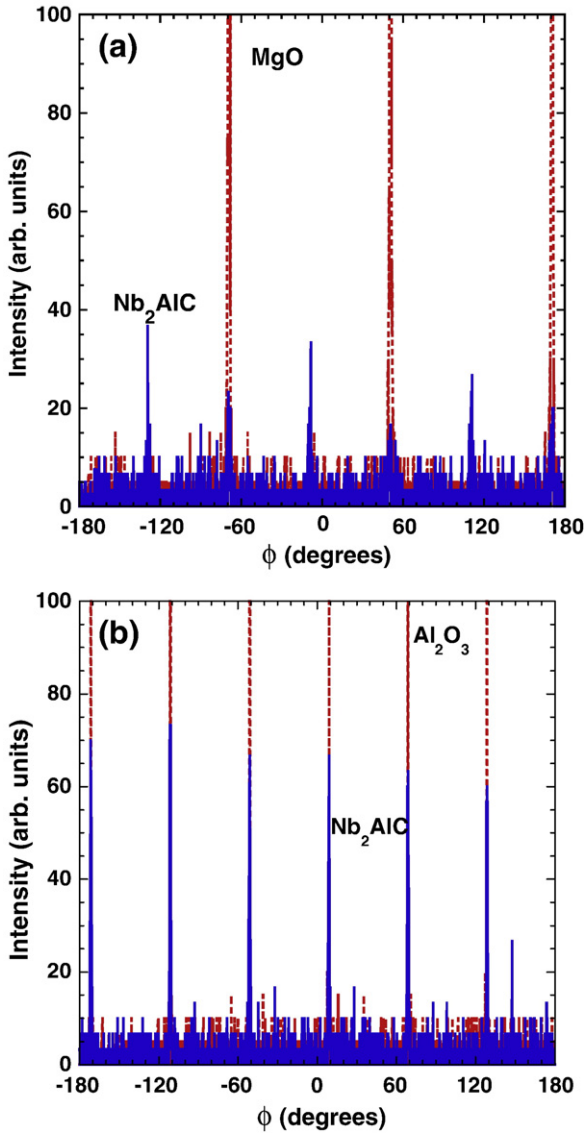

Fig. 3. ϕ scan of (103) peak of Nb_2AlC grown at 900 °C and a) (200) peak of MgO and b) (116) peak of sapphire indicating that the films are epitaxial.

settings for Nb, C, and Al were 100, 200, and 90 W, respectively, for depositions between 700 and 1000 °C (Fig. 1). At 750 °C only small amounts of Nb_2C and $Nb_5Al_3C_x$ (discussed below) were detected by XRD. Formation of *c*-axis textured Nb_2AlC was observed for deposition temperatures above 800 °C up to 950 °C along with a secondary phase of $Nb_5Al_3C_x$ with the strongest MAX phase XRD peaks at 875–900 °C.

Subsequently, a set of films were grown at 900 °C with varying carbon content with the goal of making single phase Nb_2AlC. Fig. 2 shows the XRD results for films deposited with various carbon power settings. As expected from our investigation of carbon stoichiometry of NbC and Nb_2C, the strongest diffraction peaks due to Nb_2AlC were observed at a power setting of 200 W; however, $Nb_5Al_3C_x$ was generally observed whenever Nb_2AlC was present. At the highest carbon concentration, the only instance where Nb_2AlC was found without $Nb_5Al_3C_x$, the MAX phase was the minority phase and the film was predominately Nb_2C. At low carbon concentration only the $Nb_5Al_3C_x$, NbC, and Nb_2C phases were present. Varying the deposition pressure between 5–18 mTorr had no discernable effect on the resulting films.

We were also able to grow Nb_2AlC films on (111) MgO substrates at 6 mTorr and 900 °C without a buffer layer. Despite repeated attempts, we were not able to grow Nb_2AlC films on substrates of Si, R-plane sapphire,

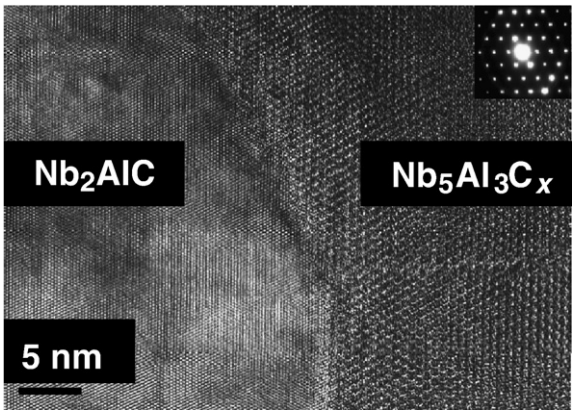

Fig. 4. Plan-view HRTEM micrograph of 270-nm thick Nb_2AlC film grown at 900 °C on *c*-axis sapphire. Two clearly different sized hexagonal structures are observed. The inset shows diffraction of the $Nb_5Al_3C_x$ phase.

or polycrystalline Al_2O_3 substrates. The lattice mismatches between Nb_2AlC and (001) α-Al_2O_3 and (111) MgO are 2.1% and 4.1%, with the films experiencing tensile and compressive strains, respectively. The former is calculated from the surface reconstruction of Al_2O_3 [15]. Both sets of films grew epitaxially, as seen from the XRD ϕ scans (Fig. 3) with in-plane relationships of $[1\bar{1}0]_{Al_2O3}||\,[100]_{Nb_2AlC}$ and $[101]_{MgO}||\,[100]_{Nb_2AlC}$.

For MAX-phase film growth a seed-layer is usually required [4,6–8]. Even when a seed layer is not deposited, a binary carbide seed layer often forms at the interface anyway [6]. In addition, (111) NbC and (001) Nb_2C have relatively small lattice mismatches of 1.8% and 0.2%, respectively. The deposition of buffer layers of (111) TiC, (111) NbC, or (001) Nb_2C on any substrates did not improve results. In fact, the quality of the films grown on *c*-axis sapphire with buffer layers, as determined from XRD, was substantially less even though both the lattice mismatch and surface roughness were minimal.

Plan-view HRTEM image of an optimized film grown on *c*-axis sapphire (Fig. 4) shows two different hexagonal structures — the one on the left is Nb_2AlC and the other has a large *a*-axis lattice parameter. Selected area electron diffraction (SAED) shown in Fig. 5 confirms that this phase (top layer) grows epitaxially *c*-axis oriented with *a*- and *c*-axis lattice constants of 7.746 Å and 5.246 Å, respectively, the latter of which gives rise to the (002) diffraction peak observed at 33.9°. While $Nb_5Al_3C_x$ does not exist in bulk [16], these lattice constants are clearly consistent with those of other $M_5A_3C_x$ compounds [5,8]. As can be seen from Fig. 5, $[110]_{Al_2O3}||\,[100]_{Nb_2AlC}||\,[110]_{Nb_5Al_3C_x}$. We speculate that since $Nb_5Al_3C_x$ forms at lower temperature as compared to that of

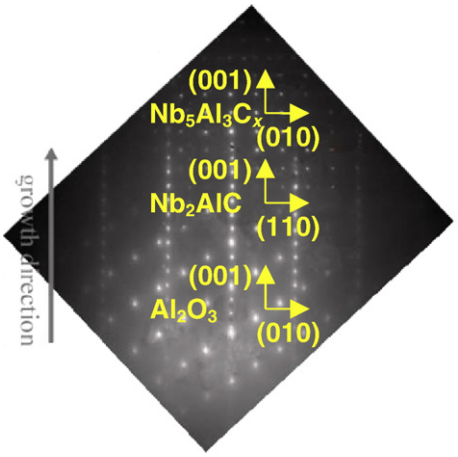

Fig. 5. Selected area electron diffraction pattern of a cross section of a 270-nm thick Nb_2AlC film grown on sapphire. There are clear the epitaxial relations among the Al_2O_3, Nb_2AlC and $Nb_5Al_3C_x$ layers.

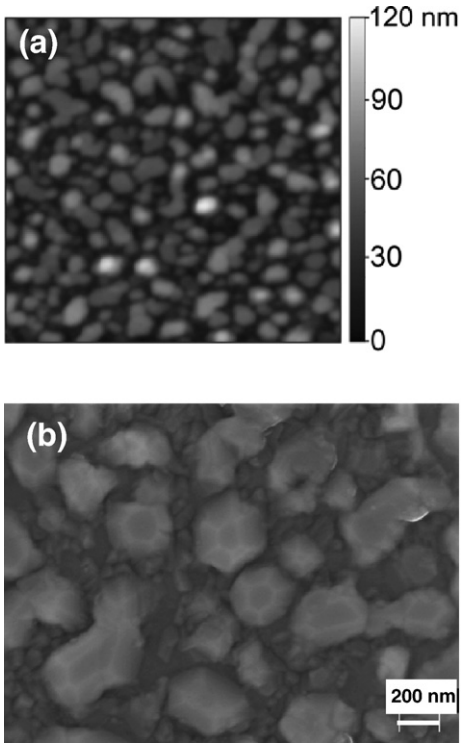

Fig. 6. a) Atomic force micrograph of a 90-nm thick Nb_2AlC (90 nm) thin film grown on sapphire. b) SEM image of the same film in which ~300 nm hexagonal features which are more clearly seen.

the MAX phase, it is the more stable phase due to the presence of lattice strain. This behavior may be similar to what happens with epitaxial films of V_2GeC which always have intergrowths of V_8C_7 [17].

Fig. 6 shows the topography of a 90-nm film grown on *c*-axis sapphire. The average surface roughness values were generally ≈15% of the total film thickness for all films. The inset of Fig. 6 shows an SEM image, which highlights the hexagonal facets ~350 nm in size and the concomitant voids of ≈175 nm. As a result of the complex surface morphology, nanoindentation and lateral force scratch testing were difficult and did not lead to reproducible results.

All first-order Raman active phonon modes associated with Nb_2AlC were observed (Table 1). There is reasonable agreement between the values found for the thin films and the calculated and measured values for bulk [18,19]. The largest difference between the bulk and film occurs for the ω_2 mode, which is a longitudinal mode in the basal plane where the atoms are some constrained due to lattice strain. There is also often a peak near 350 cm^{-1} which we attribute to $Nb_5Al_3C_x$.

The electrical resistivity ρ of all films was metal-like down to 2 K (Fig. 7). The room-temperature value of ρ in the stoichiometric films was about twice that of the bulk [11] even though the residual resistivity ratios [ρ(300 K)/ρ(4 K)] were about the same at ~2.5. This suggests that unlike the Ti_2GeC system [10], there is measurable anisotropy in the conductivity. The lower right inset in Fig. 7 shows the very low-temperature resistivity of the film with a superconducting transition at a critical temperature T_c of 440 mK. In our previous

Table 1
Measured and calculated energies of the first order Raman modes of Nb_2AlC

	Raman shift (cm^{-1})				
	ω_1	ω_2	ω_3	ω_4	References
Film	148	198	184	270	This work
Bulk	149.4	~211	~190	262.8	[18]
Calculated	148	197.7	181.5	268.3	[18]
Calculated	144	211	193	251	[19]

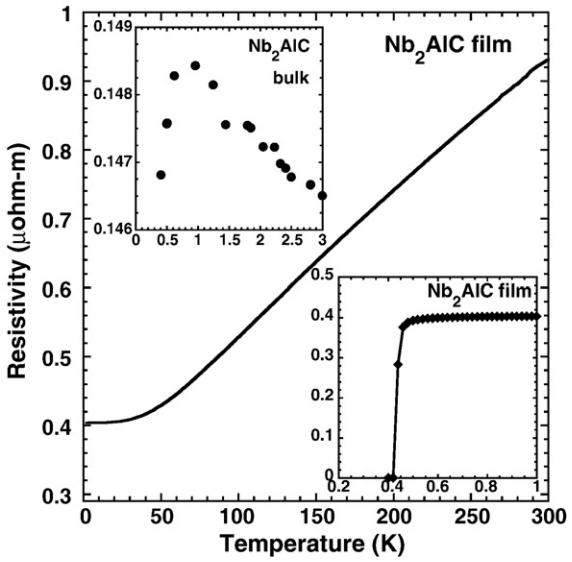

Fig. 7. Electrical resistivity of Nb_2AlC thin film showing metal-like conduction. The lower right inset shows a superconducting transition of 440 mK for the thin film. The upper left inset shows a partial superconducting transition estimated to be 430 mK for the bulk.

study [11], transport measurements were performed down only to 5 K; re-measuring the same Nb_2AlC bulk sample to lowest temperatures revealed the onset of superconductivity (upper left), with an estimated critical temperature of ≈430 mK. This suggests that the carbon stoichiometry of the films was rather close to that of the bulk, since it is well known that the T_c of niobium carbide depends rather sensitively on the carbon content [20].

4. Conclusions

In summary, we grew epitaxial thin films of Nb_2AlC on (001) sapphire and (111) MgO with and without binary carbide buffer layers. The best results were obtained on *c*-axis sapphire at 900 °C without the use of buffer layers. All films contained intergrowths of a new epitaxial phase $Nb_5Al_3C_x$. Film roughness was approximately 15% the film thickness. The resistivity was metal-like and appears to have weak anisotropy. A superconducting transition was found at 440 mK.

Acknowledgement

This work was funded by the National Science Foundation grants DMR-0503711 and MRSEC 0520471.

References

[1] M.W. Barsoum, Prog. Solid State Chem. 28 (2000) 201.
[2] M.W. Barsoum, M. Radovic, in: F. Buschow, Kramer, Mahajan, Veyssiere (Eds.), Encyclopedia of Materials Science and Technology, Elsevier, 2006, p. 16.
[3] M.W. Barsoum, M. Radovic, in: F. Buschow, Kramer, Mahajan, Veyssiere (Eds.), Encyclopedia of Materials Science and Technology, Elsevier, 2006, p. 11.
[4] J.P. Palmquist, U. Jansson, T. Seppanen, P.O.A. Persson, J. Birch, L. Hultman, P. Isberg, Appl. Phys. Lett. 81 (2002) 835.
[5] J.P. Palmquist, S. Li, P.O.A. Persson, J. Emmerlich, O. Wilhemsson, H. Högberg, M.I. Katsnelson, B. Johansson, R. Ahujia, O. Eriksson, L. Hultman, U. Jansson, Phys. Rev. B 70 (2004) 165401.
[6] J. Emmerlich, J.-P. Palmquist, H. Hogberg, J.M. Molina-Aldareguia, Z. Czigany, P.O. Persson, U. Jansson, L. Hultman, J. Appl. Phys. 96 (2004) 4817.
[7] O. Wilhelmsson, J.-P. Palmquist, T. Nyberg, U. Jansson, Appl. Phys. Lett. 85 (2004) 1066.
[8] H. Högberg, P. Eklund, J. Emmerlich, J. Birch, L. Hultman, J. Mater. Res. 20 (2005) 779.
[9] H. Högberg, L. Hultman, J. Emmerlich, T. Joelsson, P. Eklund, J.M. Molina-Aldareguia, J.P. Palmquist, O. Wilhelmsson, U. Jansson, Surf. Coat. Technol. 193 (2005) 6.
[10] T.H. Scabarozi, P. Eklund, J. Emmerlich, H. Högberg, T. Meehan, P. Finkel, M.W. Barsoum, J.D. Hettinger, L. Hultman, S.E. Lofland, Solid State Commun. 146 (2008) 498.
[11] J.D. Hettinger, S.E. Lofland, P. Finkel, T. Meehan, J. Palma, K. Harrell, S. Gupta, A. Ganguly, T. El-Raghy, M.W. Barsoum, Phys. Rev. B 72 (2005) 115120.
[12] P. Finkel, B. Seaman, K. Harrell, J. Palma, J.D. Hettinger, S.E. Lofland, A. Ganguly, M.W. Barsoum, Z. Sun, S. Li, R. Ahuja, Phys. Rev. B 70 (2004) 085104.
[13] P. Finkel, M.W. Barsoum, J.D. Hettinger, S.E. Lofland, H.I. Yoo, Phys. Rev. B 67 (2003) 235108.
[14] S.E. Lofland, J.D. Hettinger, T. Meehan, A. Bryan, P. Finkel, S. Gupta, M.W. Barsoum, G. Hug, Phys. Rev. B 74 (2006) 1.
[15] G. Renaud, Surf. Sci. Rep. 32 (1998) 1.
[16] A.I. Gusev, Russ. Chem. Rev. 95 (1996) 379.
[17] O. Wilhelmsson, P. Eklund, H. Högberg, L. Hultman, U. Jansson, Acta Mater. 56 (2008) 2563.
[18] J.E. Spanier, S. Gupta, M. Amer, M.W. Barsoum, Phys. Rev. B 71 (2005) 012103.
[19] O.D. Leaffer, S. Gupta, M.W. Barsoum, J.E. Spanier, J. Mater. Res. 22 (2007) 2651.
[20] A.L. Giorgi, E.G. Szklarz, E.K. Storms, A.L. Bowman, B.T. Matthias, Phys. Rev. 125 (1962) 837.